THE ELECTROMAGNETIC RESPONSE OF A METAMATERIAL SLAB IN THE CASE OF NORMAL INCIDENCE

A. D. Scher and E. F. Kuester

Department of Electrical and Computer Engineering
University of Colorado at Boulder
Boulder, CO 80309, USA

Abstract—In this paper, we analyze the electromagnetic response of a metamaterial slab in the case of normal incidence using the point-dipole interaction model and an expansion of polarization by eigenmodes. The problem is simplified by assuming that the lattice dimensions are smaller than a half wavelength and invoking the nearest neighbor approximation. In this manner, we find the structure supports three modes: an ordinary mode and two extraordinary modes. A systematic method is presented to find the scattering from the slab, and the results are confirmed by full wave simulation using Ansoft HFSS.

1. INTRODUCTION

The metamaterial slab, which is finite in the direction normal to the surface and infinite (or electrically very large) in the transverse directions, is an important structure to study with a number of applications. Perhaps one of the most well-known and referenced applications is the "perfect lens" [1], which is a slab with $\mu_{r,eff} = \varepsilon_{r,eff} = -1$ that can theoretically achieve perfect imaging by reproducing both the propagating and evanescent waves associated with a flat object. While such a perfect lens has inevitably been shown to be impossible to reach in practice, a real slab can certainly approach the theoretical limit [2–6]. For microwave applications, a metamaterial slab with a near-zero index of refraction $n_{eff} = \sqrt{\varepsilon_{r,eff}\mu_{r,eff}} \approx 0$ can be used to increase the directivity of an antenna by blocking obliquely incident waves [7–10]. Metamaterial slabs have also been proposed

as a means of miniaturizing resonant cavities [11–13] and for making small resonant absorbers [14]. Another major application is material characterization, in which the measured scattering from a metamaterial slab under test is used to infer the effective medium parameters of the composite itself [15–18].

Of course, a metamaterial slab is not really an ideal continuum with well-defined boundaries, but a number of planar arrays of scatterers cascaded along the array axis. Treating such a structure as an effective medium requires careful consideration. For one, the effective thickness t_s of the slab is seemingly ambiguous, even though a common and intuitive choice is to simply assume the effective thickness is $t_s = d \times N$, where d is the lattice constant along the array axis and N is the number of lattice planes. Also, due to the inherent structural asymmetry at particle positions near the surface, the local electromagnetic fields and currents at these positions naturally differ from those in the bulk of the medium. Consequently, the polarization distribution of the discrete scatterers can vary rapidly and even oscillate within a thin transition layer near the surface [19–23]. Various models for the air-metamaterial interface have been proposed to account for surface effects, such as a thin effective Drude transition layer [16] and a pair of electric and magnetic effective surface susceptibilities, which lead to the generalized sheet transition conditions [24].

Besides the surface effects, there still seems to be no clear consensus on how to properly assign the effective parameters $\mu_{r,\mathit{eff}}$ and $\varepsilon_{r,\mathit{eff}}$ to the bulk itself. In the long-wavelength limit, the classic Clausius-Mossotti relations relate the polarizabilities of the scatterers to the effective medium parameters. However, at higher frequencies in which the inhomogenieties become sizable compared to the wavelength inside the medium, the simple Clausius-Mossotti approximation can break down, and a nonlocal (i.e., spatially dispersive) characterization of the bulk response may be required. For such a case, a variety of homogenization schemes have been proposed (e.g., see Refs. [16, 25–27]).

It is therefore important to examine the electromagnetic response of a metamaterial slab in an analytical way that is independent of the effective medium description altogether. Analytic solutions are useful as a benchmark to compare with the myriad of effective medium and surface models proposed in the literature. For design purposes they promote a better understanding and insight into the scattering problem. In this paper, we formulate an analytic solution by employing the point-interaction model in which each individual scatterer is considered as a simple responding point-dipole. This model

(also sometimes called the "microscopic model") has been a useful and popular tool for analyzing scattering problems for decades. For example, Ewald employed the model in is his pioneering work on X-ray diffraction [28] and Sivukhin used it to systematically study the properties of clean crystalline surfaces [23].

The point-dipole interaction model was also utilized in an influential 1969 paper by Mahan and Obermair [29], in which the reflectivity of a crystalline half-space in the case of normal incidence was solved for by expressing the discrete polarization distribution as a superposition of the infinite crystal polarization eigenmodes. Later, Philpott extended this work to the case of oblique incidence for both semi-infinite crystals [30, 31] and slabs of finite thickness [32]. In more recent years, the eigenmode approach has been expanded and adapted to the analysis of artificial crystals and metamaterials (e.g., see Refs. [16, 25, 33–42]).

In this paper, we apply the eigenmode approach to the specific problem of scattering from a metamaterial slab in the case of normal incidence. In some sense, this can be considered as an expansion of Philpott's work on purely-dielectric slabs [32] to the more general case of a magnetodielectric slab. In our analysis, we consider only nearest-neighbor near-field interactions, which offers a good balance between numerical accuracy and simplicity. With this, we shall find that the dispersion relation contains three roots, which characterize the propagation of an ordinary mode and two extraordinary modes. More recently Simovski et al. derived the dispersion relation for a magnetodielectric crystal (akin to what we are considering here) in two alternative equivalent forms [16, 40]. However, in these works the authors ignore all near-field interactions between neighboring planes. While this is adequate for investigating bulk properties, we include nearest-neighbor interactions, because, as Berman demonstrated for the purely-dielectric case [22], such near-field interactions are crucial for accurately capturing the detailed surface effects.

2. PROBLEM FORMULATION

Consider a transverse electromagnetic (TEM_z) plane wave with wave vector $\mathbf{k} = k_0 \hat{\mathbf{a}}_z$ normally incident from free-space upon a metamaterial slab composed of a periodic arrangement of scatterers arranged in the nodes an $a \times b \times d$ orthorhombic lattice, as shown in Fig. 1. The lattice is of infinite extent along the x- and y-directions but contains a finite number of periods N along the z-direction. The sites of the lattice are taken to be

$$\mathbf{R}_{as,bl,dn} = \hat{\mathbf{a}}_x as + \hat{\mathbf{a}}_y bl + \hat{\mathbf{a}}_z dn \tag{1}$$
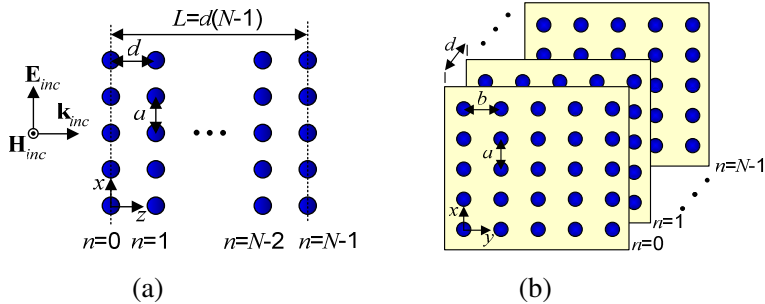
Figure 1. Metamaterial slab excited by a normally incident plane wave. Shown here are views of the (a) xz-plane cross section and (b) one point perspective in the transverse plane.

where $s, l = 0, \pm 1, \pm 2, \ldots$, and $n = 0, 1, 2, \ldots, N - 1$. Since we are interested in the structure's response at frequencies below the Bragg diffraction regime, we restrict the dimensions of the lattice to be smaller than a wavelength in free-space, i.e., $k_0 \max(a, b, d) < 2\pi$. Note that in the more general case of oblique incidence (not considered here), which my involve angles of incidence approach grazing, the dimensions of the lattice would have to be smaller than a half wavelength in free-space to avoid Bragg diffraction.

In the point-dipole approximation the response of a given scatterer is characterized solely by its electric and magnetic polarizability dyadics, denoted $\overleftrightarrow{\boldsymbol{\alpha}}_E(\omega)$ and $\overleftrightarrow{\boldsymbol{\alpha}}_M(\omega)$, respectively. In this work, we focus on biaxially anisotropic particles exhibiting no magnetoelectric coupling, which corresponds to polarizability dyadics with non-zero elements exclusively along the diagonal, i.e., $\overleftrightarrow{\boldsymbol{\alpha}}_E = \hat{\mathbf{a}}_x \hat{\mathbf{a}}_x \alpha_E^{xx} + \hat{\mathbf{a}}_y \hat{\mathbf{a}}_y \alpha_E^{yy} + \hat{\mathbf{a}}_z \hat{\mathbf{a}}_z \alpha_E^{zz}$ and $\overleftrightarrow{\boldsymbol{\alpha}}_M = \hat{\mathbf{a}}_x \hat{\mathbf{a}}_x \alpha_M^{xx} + \hat{\mathbf{a}}_y \hat{\mathbf{a}}_y \alpha_M^{yy} + \hat{\mathbf{a}}_z \hat{\mathbf{a}}_z \alpha_M^{zz}$. These polarizability dyadics characterize scatterers with geometries exhibiting mirror symmetries about the three principle planes (i.e., the xy-, xz-, and yz-planes). The consideration of more complicated particles such as split-ring resonators which exhibit cross-polarization and magnetoelectric coupling are beyond the scope of this work. In Ref. [15], we showed how to extract the elements of the polarizability dyadics from the measured or simulated scattering parameters of a single planar array of such scatterers.

With no further loss in generality, let us assume that the incident plane wave is polarized along the x-axis, such that the incident electric field $\mathbf{E}_{inc}$ and incident magnetic field $\mathbf{H}_{inc}$ take the form:

$$\mathbf{E}_{inc} = \hat{\mathbf{a}}_x E_{inc,x} e^{-jk_0 z} \tag{2}$$

$$\mathbf{H}_{inc} = \hat{\mathbf{a}}_y \frac{E_{inc,x}}{\eta_0} e^{-jk_0 z} \tag{3}$$

where $E_{inc,x}$ is the amplitude of the incident electric field and $\eta_0 = \sqrt{\mu_0/\varepsilon_0}$ is the wave impedance of free space. In the point-dipole approximation, the incident wave excites a distribution of oscillating point-electric and point-magnetic dipole moments situated at the nodes of the lattice, denoted $\mathbf{p}_{s,l,n} \equiv \mathbf{p}(as, bl, dn)$ and $\mathbf{m}_{s,l,n} \equiv \mathbf{m}(as, bl, dn)$, respectively. Because the system obeys translational invariance in the xy-plane, the electric and magnetic dipole distributions take the form $\mathbf{p}_{s,l,n} = \mathbf{p}_n$ and $\mathbf{m}_{s,l,n} = \mathbf{m}_n$, where $\mathbf{p}_n \equiv \mathbf{p}_{n,0,0}$ and $\mathbf{m}_n \equiv \mathbf{m}_{n,0,0}$ denote the electric and magnetic dipole moments of the particle located at the origin of lattice plane $z = dn$, respectively.

To find the distributions $\{\mathbf{p}_n\}$ and $\{\mathbf{m}_n\}$, we take the local-field approach and write the following system of equations, which govern the response for each scatterer positioned along the z-axis:

$$\mathbf{p}_{n'} = \varepsilon_0 \overset{\leftrightarrow}{\boldsymbol{\alpha}}_E \cdot \mathbf{E}_{loc,n'}, \qquad \forall \, n' = 0, 1, 2, \ldots, N-1 \tag{4}$$

$$\mathbf{m}_{n'} = \mu_0^{-1} \overset{\leftrightarrow}{\boldsymbol{\alpha}}_M \cdot \mathbf{B}_{loc,n'}, \quad \forall \, n' = 0, 1, 2, \ldots, N-1, \tag{5}$$

where $\mathbf{E}_{loc,n'}$ and $\mathbf{B}_{loc,n'}$ denote the local electric and magnetic fields acting on the scatterer at site $(0, 0, n')$; this site corresponds to the origin of the $a \times b$ array in plane $z = dn'$. The local electric field $\mathbf{E}_{loc,n'}$ is found by superposing the incident electric field at site $(0, 0, n')$ and the induced electric fields at that site produced by all other scatters with indices $(s, l, n) \neq (0, 0, n')$; a dual statement holds for the local magnetic field $\mathbf{B}_{loc,n'}$. Taking a planewise summation approach (akin to that taken in Refs. [29–32, 39, 43]), the above statements can be expressed as the following:

$$\mathbf{E}_{loc,n'} = \frac{1}{(ab)^{3/2}\varepsilon_0} \left(\sum_{n=0}^{N-1} \overset{\leftrightarrow\text{TEM}_z}{\mathbf{C}}_{n-n'} \cdot \mathbf{p}_n - \frac{1}{c_0} \sum_{n=0}^{N-1} \overset{\leftrightarrow\text{TEM}_z}{\mathbf{D}}_{n-n'} \cdot \mathbf{m}_n \right) + \mathbf{E}_{inc,n'} \tag{6}$$

$$\mathbf{B}_{loc,n'} = \frac{\mu_0}{(ab)^{3/2}} \left(c_0 \sum_{n=0}^{N-1} \overset{\leftrightarrow\text{TEM}_z}{\mathbf{D}}_{n-n'} \cdot \mathbf{p}_n + \sum_{n=0}^{N-1} \overset{\leftrightarrow\text{TEM}_z}{\mathbf{C}}_{n-n'} \cdot \mathbf{m}_n \right) + \mathbf{B}_{inc,n'} \tag{7}$$

where c_0 is the speed of light in vacuum, $\mathbf{E}_{inc,n'} \equiv \mathbf{E}_{inc}(0, 0, dn')$, $\mathbf{B}_{inc,n'} \equiv \mathbf{B}_{inc}(0, 0, dn')$, and $\overset{\leftrightarrow\text{TEM}_z}{\mathbf{C}}_{n-n'}$ and $\overset{\leftrightarrow\text{TEM}_z}{\mathbf{D}}_{n-n'}$ denote the co-field and cross-field planar interaction dyadics, respectively. By definition, the co-field planar interaction dyadic $\overset{\leftrightarrow\text{TEM}_z}{\mathbf{C}}_{n-n'}$ quantifies the contribution to the local electric (magnetic) field at site $(0, 0, n')$ produced by an $a \times b$ array of electric (magnetic) dipoles located in

plane $z = dn$:

$$
\overset{\leftrightarrow}{\mathbf{C}}_{n-n'}^{\mathrm{TEM}_z} \equiv
\begin{cases}
(ab)^{3/2} \sum\limits_{s=-\infty}^{\infty} \sum\limits_{l=-\infty}^{\infty} \overset{\leftrightarrow}{\mathbf{G}}^{(1)} \left(\mathbf{R}_{as,bl,d(n-n')} \right), \ n \neq n' \\[2ex]
(ab)^{3/2} \sum\limits_{(s,l)\neq(0,0)} \overset{\leftrightarrow}{\mathbf{G}}^{(1)} \left(\mathbf{R}_{as,bl,0} \right), \ n = n'
\end{cases}
\tag{8}
$$

where the symbol $\sum\limits_{(s,l)\neq(0,0)} (\cdot)$ denotes a double infinite sum over all indices $(s, l) \neq (0, 0)$; and $\overset{\leftrightarrow}{\mathbf{G}}^{(1)} (\mathbf{R}_{x,y,z})$ is the normalized dyadic Green's function of free space describing the electric (magnetic) field evaluated at position $\mathbf{R}_{x,y,z} = \hat{\mathbf{a}}_x x + \hat{\mathbf{a}}_y y + \hat{\mathbf{a}}_z z$ as produced by a single electric (magnetic) dipole located at the coordinate origin:

$$
\overset{\leftrightarrow}{\mathbf{G}}^{(1)} (\mathbf{R}_{x,y,z}) = \frac{1}{4\pi} \left(k_0^2 \overset{\leftrightarrow}{I} + \boldsymbol{\nabla}\boldsymbol{\nabla} \right) \frac{e^{-jk_0|R_{x,y,z}|}}{|\mathbf{R}_{x,y,z}|}
\tag{9}
$$

where $\overset{\leftrightarrow}{I} \equiv \hat{\mathbf{a}}_x \hat{\mathbf{a}}_x + \hat{\mathbf{a}}_y \hat{\mathbf{a}}_y + \hat{\mathbf{a}}_z \hat{\mathbf{a}}_z$. In our notation, the terms $\overset{\leftrightarrow}{\mathbf{G}}^{(1)} (\mathbf{R}_{as,bl,d(n-n')})$ and $\overset{\leftrightarrow}{\mathbf{G}}^{(1)} (\mathbf{R}_{as,bl,0})$, which appear in Eq. (8), imply that the differential operation given by Eq. (9) is performed before the specified change of variables; $(x, y, z) = (as, bl, dn - dn')$ and $(x, y, z) = (as, bl, 0)$, respectively. The cross-field planar interaction dyadic $\overset{\leftrightarrow}{\mathbf{D}}_{n-n'}^{\mathrm{TEM}_z}$ quantifies the contribution to the local magnetic (electric) field at site $(0, 0, n')$ produced by an $a \times b$ array of electric (magnetic) dipoles located in plane $z = dn$:

$$
\overset{\leftrightarrow}{\mathbf{D}}_{n-n'}^{\mathrm{TEM}_z} \equiv
\begin{cases}
(ab)^{3/2} \sum\limits_{s=-\infty}^{\infty} \sum\limits_{l=-\infty}^{\infty} \overset{\leftrightarrow}{\mathbf{G}}^{(2)} \left(\mathbf{R}_{as,bl,d(n-n')} \right), \ n \neq n' \\[2ex]
(ab)^{3/2} \sum\limits_{(s,l)\neq(0,0)} \overset{\leftrightarrow}{\mathbf{G}}^{(2)} (\mathbf{R}_{as,bl,0}), \ n = n'
\end{cases}
\tag{10}
$$

where $\overset{\leftrightarrow}{\mathbf{G}}^{(2)} (\mathbf{R}_{x,y,z})$ is the normalized dyadic Green's functions of free space describing the magnetic (electric) field evaluated at position $\mathbf{R}_{x,y,z} = \hat{\mathbf{a}}_x x + \hat{\mathbf{a}}_y y + \hat{\mathbf{a}}_z z$ as produced by a single electric (magnetic) dipole located at the coordinate origin:

$$
\overset{\leftrightarrow}{\mathbf{G}}^{(2)} (\mathbf{R}_{x,y,z}) = \frac{-jk_0}{4\pi} \left(\boldsymbol{\nabla} \times \overset{\leftrightarrow}{I} \right) \frac{e^{-jk_0|R_{x,y,z}|}}{|\mathbf{R}_{x,y,z}|}
\tag{11}
$$

By definition, both $\overset{\leftrightarrow}{\mathbf{C}}_{n-n'}^{\mathrm{TEM}_z}$ and $\overset{\leftrightarrow}{\mathbf{D}}_{n-n'}^{\mathrm{TEM}_z}$ are dimensionless quantities. The multiplying factors, $(ab)^{-3/2} \varepsilon_0^{-1}$ and $(ab)^{-3/2} \mu_0$, on the right sides of Eqs. (6) and (7), respectively, serve as normalization factors.

In matrix form, the planar interaction dyadics can be written in terms of their components:

$$
\overset{\leftrightarrow}{\mathbf{C}}{}^{\mathrm{TEM}_z}_{n-n'} = \begin{bmatrix} C^{\mathrm{TEM}_z,xx}_{n-n'} & C^{\mathrm{TEM}_z,xy}_{n-n'} & C^{\mathrm{TEM}_z,xz}_{n-n'} \\ C^{\mathrm{TEM}_z,yx}_{n-n'} & C^{\mathrm{TEM}_z,yy}_{n-n'} & C^{\mathrm{TEM}_z,yz}_{n-n'} \\ C^{\mathrm{TEM}_z,zx}_{n-n'} & C^{\mathrm{TEM}_z,zy}_{n-n'} & C^{\mathrm{TEM}_z,zz}_{n-n'} \end{bmatrix} \tag{12}
$$

$$
\overset{\leftrightarrow}{\mathbf{D}}{}^{\mathrm{TEM}_z}_{n-n'} = \begin{bmatrix} D^{\mathrm{TEM}_z,xx}_{n-n'} & D^{\mathrm{TEM}_z,xy}_{n-n'} & D^{\mathrm{TEM}_z,xz}_{n-n'} \\ D^{\mathrm{TEM}_z,yx}_{n-n'} & D^{\mathrm{TEM}_z,yy}_{n-n'} & D^{\mathrm{TEM}_z,yz}_{n-n'} \\ D^{\mathrm{TEM}_z,zx}_{n-n'} & D^{\mathrm{TEM}_z,zy}_{n-n'} & D^{\mathrm{TEM}_z,zz}_{n-n'} \end{bmatrix} \tag{13}
$$

where,

$$
\begin{aligned}
&\mathbf{C}^{\mathrm{TEM}_z,uv}_{n-n'}(k_0,a,b,d) \\
&= \begin{cases} (ab)^{3/2}\,\hat{\mathbf{a}}_u \cdot \displaystyle\sum_{s=-\infty}^{\infty}\sum_{l=-\infty}^{\infty} \overset{\leftrightarrow}{\mathbf{G}}{}^{(1)}\left(\mathbf{R}_{as,bl,d(n-n')}\right)\cdot\hat{\mathbf{a}}_v, \ n \neq n' \\ (ab)^{3/2}\,\hat{\mathbf{a}}_u \cdot \displaystyle\sum_{(s,l)\neq(0,0)} \overset{\leftrightarrow}{\mathbf{G}}{}^{(1)}\left(\mathbf{R}_{as,bl,0}\right)\cdot\hat{\mathbf{a}}_v, \ n = n' \end{cases}
\end{aligned} \tag{14}
$$

$$
\begin{aligned}
&D^{\mathrm{TEM}_z,uv}_{n-n'}(k_0,a,b,d) \\
&= \begin{cases} (ab)^{3/2}\,\hat{\mathbf{a}}_u \cdot \displaystyle\sum_{s=-\infty}^{\infty}\sum_{l=-\infty}^{\infty} \overset{\leftrightarrow}{\mathbf{G}}{}^{(2)}\left(\mathbf{R}_{as,bl,d(n-n')}\right)\cdot\hat{\mathbf{a}}_v, \ n \neq n' \\ (ab)^{3/2}\,\hat{\mathbf{a}}_u \cdot \displaystyle\sum_{(s,l)\neq(0,0)} \overset{\leftrightarrow}{\mathbf{G}}{}^{(2)}\left(\mathbf{R}_{as,bl,0}\right)\cdot\hat{\mathbf{a}}_v, \ n = n' \end{cases}
\end{aligned} \tag{15}
$$

for u, $v = x$, y, or z. Using Eq. (14), we find that out of the nine components of $\overset{\leftrightarrow}{\mathbf{C}}{}^{\mathrm{TE}_z}_{n-n'}$ which appear in the right-hand side of Eq. (12), the following six components are equal to zero: $C^{\mathrm{TEM}_z,xy}_{n-n'} = C^{\mathrm{TEM}_z,yx}_{n-n'} = C^{\mathrm{TEM}_z,zy}_{n-n'} = C^{\mathrm{TEM}_z,yz}_{n-n'} = C^{\mathrm{TEM}_z,xz}_{n-n'} = C^{\mathrm{TEM}_z,zx}_{n-n'} = 0$. We can therefore rewrite $\overset{\leftrightarrow}{\mathbf{C}}{}^{\mathrm{TEM}_z}_{n-n'}$ as the following symmetric matrix in terms of only $C^{\mathrm{TEM}_z,xx}_{n-n'}$, $C^{\mathrm{TEM}_z,yy}_{n-n'}$ and $C^{\mathrm{TEM}_z,zz}_{n-n'}$:

$$
\overset{\leftrightarrow}{C}{}^{\mathrm{TEM}_z}_{n-n'} = \begin{bmatrix} C^{\mathrm{TEM}_z,xx}_{n-n'} & 0 & 0 \\ 0 & C^{\mathrm{TEM}_z,yy}_{n-n'} & 0 \\ 0 & 0 & C^{\mathrm{TEM}_z,zz}_{n-n'} \end{bmatrix} \tag{16}
$$

We leave the details of $C^{\mathrm{TEM}_z,xx}_{n-n'}$ and $C^{\mathrm{TEM}_z,yy}_{n-n'}$ to the next section ($C^{\mathrm{TEM}_z,zz}_{n-n'}$ is not needed for our purposes, since, as will be shown, the polarization distribution has no z-component). Using Eq. (15), we find

that out of the nine components of $\overset{\leftrightarrow}{\mathbf{D}}{}_{n-n'}^{\mathrm{TEM}_z}$ which appear on the right-hand side of Eq. (13), the following seven components are equal to zero: $D_{n-n'}^{\mathrm{TEM}_z,xx} = D_{n-n'}^{\mathrm{TEM}_z,zz} = D_{n-n'}^{\mathrm{TEM}_z,yy} = D_{n-n'}^{\mathrm{TEM}_z,zx} = D_{n-n'}^{\mathrm{TEM}_z,xz} = D_{n-n'}^{\mathrm{TEM}_z,yz} = D_{n-n'}^{\mathrm{TEM}_z,zy} = 0$. From the remaining two components, only one is independent; allowing us to rewrite $\overset{\leftrightarrow}{\mathbf{D}}{}_{n-n'}^{\mathrm{TE}_z}$ as the following skew-symmetric matrix in terms of only $D_{n-n'}^{\mathrm{TEM}_z,yx}$:

$$
\overset{\leftrightarrow}{\mathbf{D}}{}_{n-n'}^{\mathrm{TEM}_z} = \begin{bmatrix} 0 & -D_{n-n'}^{\mathrm{TEM}_z,yx} & 0 \\ D_{n-n'}^{\mathrm{TEM}_z,yx} & 0 & 0 \\ 0 & 0 & 0 \end{bmatrix} \tag{17}
$$

We leave the details of $D_{n-n'}^{\mathrm{TEM}_z,yx}$ to the next section.

By substituting Eqs. (6), (7), (16), and (17), into Eqs. (4) and (5), we find that the only non-zero vector components of $\mathbf{p}_n$ and $\mathbf{m}_n$ are those that lie along the same directions as the incident field vectors, $\mathbf{E}_{inc,n'}$ and $\mathbf{B}_{inc,n'}$, respectively. Hence, we may write $\mathbf{p}_n = \hat{\mathbf{a}}_x p_n^{(x)}$ and $\mathbf{m}_n = \hat{\mathbf{a}}_y m_n^{(y)}$. Consequently, it follows from Eqs. (6) and (7) that the local electric and magnetic fields, $\mathbf{E}_{loc,n'}$ and $\mathbf{B}_{loc,n'}$, must also be polarized along the same directions as the incident field vectors $\mathbf{E}_{inc,n'}$ and $\mathbf{B}_{inc,n'}$, respectively, i.e. $\mathbf{E}_{loc,n'} = \hat{\mathbf{a}}_x \mathbf{E}_{loc,n}^{(x)}$ and $\mathbf{B}_{loc,n'} = \hat{\mathbf{a}}_y B_{loc,n}^{(y)}$. Substituting Eqs. (2), (3), (6), (7), and (16)–(17) into Eqs. (4) and (5) yields the following set of $2N$ coupled local-field equations, which are to be solved for the $2N$ unknowns, $p_n^{(x)}$ and $m_n^{(y)}$; $n = 0, 1, 2, \ldots, N-1$:

$$
p_{n'}^{(x)} = \frac{\alpha_E^{xx}}{(ab)^{3/2}} \left[\sum_{n=0}^{N-1} p_n^{(x)} C_{n-n'}^{\mathrm{TEM}_z,xx} + \frac{1}{c_0} \sum_{n=0}^{N-1} m_n^{(y)} D_{n-n'}^{\mathrm{TEM}_z,yx} \right]
$$
$$
+ \alpha_E^{xx} \varepsilon_0 E_{inc,x} e^{-jk_0 dn'}, \ \forall \ n' = 0, 1, 2, \ldots, N-1 \tag{18}
$$

$$
m_{n'}^{(y)} = \frac{\alpha_M^{yy}}{(ab)^{3/2}} \left[c_0 \sum_{n=0}^{N-1} p_n^{(x)} D_{n-n'}^{\mathrm{TEM}_z,yx} + \sum_{n=0}^{N-1} m_n^{(y)} C_{n-n'}^{\mathrm{TEM}_z,yy} \right]
$$
$$
+ \alpha_M^{yy} \frac{E_{inc,x}}{\eta_0} e^{-jk_0 dn'}, \ \forall \ n' = 0, 1, 2, \ldots, N-1 \tag{19}
$$

3. THE PLANAR INTERACTION CONSTANTS

A key to solving Eqs. (18) and (19) resides in calculating $C_{n-n'}^{\mathrm{TEM}_z,xx}$, $C_{n-n'}^{\mathrm{TEM}_z,yy}$ and $D_{n-n'}^{\mathrm{TEM}_z,xy}$. In Section 4 of Ref. [44], we examined a metamaterial of infinite extent (as opposed to a slab of finite extent

in one direction, as we are doing here), which involved considering the same interaction terms. In this reference, it was found to be useful to expand these interaction terms into their short-range (SR) and long-range (LR) components. For instance, the term $C_{n-n'}^{\mathrm{TEM}_z,xx}$ can be expanded as:

$$C_{n-n'}^{\mathrm{TEM}_z,xx}(k_0,a,b,d) \equiv C_{n-n',\mathrm{SR}}^{\mathrm{TEM}_z,xx}(k_0,a,b,d) + C_{n-n',\mathrm{LR}}^{\mathrm{TEM}_z,xx}(k_0,a,b,d) \tag{20}$$

where the respective SR and LR components of $C_{n-n'}^{\mathrm{TEM}_z,xx}$ are given by:

$$C_{n-n',\mathrm{LR}}^{\mathrm{TEM}_z,xx}(k_0,a,b,d) = -j\frac{k_0\,(ab)^{1/2}}{2}e^{-j|n-n'|k_0 d} \tag{21}$$

$$C_{n-n',\mathrm{SR}}^{\mathrm{TEM}_z,xx}(k_0,a,b,d)$$

$$= \begin{cases} \sum\limits_{(s,l)\neq(0,0)} \dfrac{(ab)^{1/2}\left[k_0^2-(2\pi s/a)^2\right]}{2\sqrt{\left(\frac{2\pi s}{a}\right)^2+\left(\frac{2\pi l}{b}\right)^2-k_0^2}}e^{-|n'-n|d\sqrt{\left(\frac{2\pi s}{a}\right)^2+\left(\frac{2\pi l}{b}\right)^2-k_0^2}}, & n\neq n' \\[4mm] \mathrm{Re}\left\{C_0^{\mathrm{TEM}_z,xx}\right\} + j\,(ab)^{3/2}\dfrac{k_0^3}{6\pi}, & n=n' \end{cases} \tag{22}$$

The double sum in Eq. (22) for $n \neq n'$ (describing short-range interplanar coupling) is rapidly convergent and convenient for numerical calculation. Assuming that $k_0\max(a,b) > 2\pi$, this sum quickly decays to zero with increasing interplanar distance $|n-n'|\,d$. Physically, the terms in this sum are associated with the cut-off (evanescent) free-space modes produced by a planar array of oscillating dipoles that exist only in the near-field. For large interplanar distances $|n-n'|\,d$, the long-range term given by Eq. (21) is dominant. The intraplaner term $C_0^{\mathrm{TEM}_z,xx}$ in the second expression in Eq. (22) can be numerically calculated using the series given by Eq. (13) in Ref. [44].

By the symmetry of the problem, $C_{n-n'}^{\mathrm{TEM}_z,yy}$ is related to $C_{n-n'}^{\mathrm{TEM}_z,xx}$ by interchanging the variables a and b:

$$C_{n-n'}^{\mathrm{TEM}_z,yy}(k_0,a,b,d) = C_{n-n'}^{\mathrm{TEM}_z,xx}(k_0,b,a,d) \tag{23}$$

Hence, we may also expand $C_{n-n'}^{\mathrm{TEM}_z,yy}$ as a sum of two components, describing separately short-range (SR) and long-range (LR) interactions:

$$C_{n-n'}^{\mathrm{TEM}_z,yy}(k_0,a,b,d) \equiv C_{n-n',\mathrm{SR}}^{\mathrm{TEM}_z,yy}(k_0,a,b,d) + C_{n-n',\mathrm{LR}}^{\mathrm{TEM}_z,yy}(k_0,a,b,d)$$

$$= C_{n-n',\mathrm{SR}}^{\mathrm{TEM}_z,xx}(k_0,b,a,d) + C_{n-n',\mathrm{LR}}^{\mathrm{TEM}_z,xx}(k_0,b,a,d) \tag{24}$$

From Eq. (21), we see that the long-range component of $C_{n-n'}^{\mathrm{TEM}_z,xx}$ is invariant with respect to the interchange of variables a and b, i.e., $C_{n-n',\mathrm{LR}}^{\mathrm{TEM}_z,xx}(k_0,a,b,d) = C_{n-n',\mathrm{LR}}^{\mathrm{TEM}_z,xx}(k_0,b,a,d)$. Hence, the long-range

components of $C_{n-n'}^{\text{TEM}_z,yy}$ and $C_{n-n'}^{\text{TEM}_z,xx}$ are equal, i.e. $C_{n-n',\text{LR}}^{\text{TEM}_z,yy} = C_{n-n',\text{LR}}^{\text{TEM}_z,xx}$. From Eqs. (22) and (24), we see that the short range components of $C_{n-n'}^{\text{TEM}_z,yy}$ and $C_{n-n'}^{\text{TEM}_z,xx}$ are only equal in the case of a square lattice ($a = b$).

Finally, we expand $D_{n-n'}^{\text{TEM}_z,yx}$ as a sum of two components, describing separately short-range (SR) and long-range (LR) interactions:

$$D_{n-n'}^{\text{TEM}_z,yx}(k_0,a,b,d) \equiv D_{n-n',\text{SR}}^{\text{TEM}_z,yx}(k_0,a,b,d) + D_{n-n',\text{LR}}^{\text{TEM}_z,yx}(k_0,a,b,d) \tag{25}$$

where the respective SR and LR components of $D_{n-n'}^{\text{TEM}_z,yx}$ are given by [44]:

$$D_{n-n',\text{LR}}^{\text{TEM}_z,yx}(k_0,a,b,d) = \text{sgn}\left(n - n'\right) \frac{jk_0\left(ab\right)^{1/2}}{2} e^{-j|n-n'|k_0 d} \tag{26}$$

$$D_{n-n',\text{SR}}^{\text{TEM}_z,yx}(k_0,a,b,d)$$
$$= \text{sgn}\left(n - n'\right) \frac{jk_0\left(ab\right)^{1/2}}{2} \sum_{(s,l)\neq(0,0)} e^{-|n'-n'|d\sqrt{\left(\frac{2\pi s}{a}\right)^2+\left(\frac{2\pi l}{b}\right)^2-k_0^2}} \tag{27}$$

where $\text{sgn}(x)$ denotes the signum function ($\text{sgn}(x) = 1$ for $x > 1$, $\text{sgn}(x) = -1$ for $x < 1$, and $\text{sgn}(x) = 0$ for $x = 0$).

In general, the short-range terms, $C_{n-n',\text{SR}}^{\text{TEM}_z,xx}$, $C_{n-n',\text{SR}}^{\text{TEM}_z,yy}$ and $D_{n-n',\text{SR}}^{\text{TEM}_z,yx}$, decrease rapidly in magnitude as a function of increasing separation distance $|n - n'|d$, while the long range terms, $C_{n-n',\text{LR}}^{\text{TEM}_z,xx}$, $C_{n-n',\text{LR}}^{\text{TEM}_z,yy}$ and $D_{n-n',\text{LR}}^{\text{TEM}_z,yx}$, simply change phase. Guided by the results and discussion of Section 4 in Ref. [44], we find that to a good approximation, the SR co-field terms, $C_{n-n',\text{SR}}^{\text{TEM}_z,xx}$ and $C_{n-n',\text{SR}}^{\text{TEM}_z,yy}$, are negligible and can be set equal to zero for $|n - n'| \geq 2$. This nearest-neighbor approximation drastically simplifies our problem at the expensive of only a small loss in accuracy, and is independent on the exact nature of the scatterer. Additionally, the SR cross-field term, $D_{n-n',\text{SR}}^{\text{TEM}_z,yx}$, is negligible compared to $\left|D_{n-n',\text{LR}}^{\text{TEM}_z,yx}\right|$ for all planar indices, and can thus be set to zero altogether. In general, we find that these approximations hold valid so long as the lattice period along the normal is equal to or larger than the period along the transverse directions (i.e., $d \geq \max(a,b)$). This condition is assumed throughout the rest of the paper. Applying these approximations to Eqs. (18) and (19) results in

the following form of the local-field equations:

$$
p_{n'}^{(x)} = \frac{\alpha_E^{xx}}{(ab)^{3/2}} \left[\sum_{n=0}^{N-1} p_n^{(x)} C_{n-n',\mathrm{LR}}^{\mathrm{TEM}_z,xx} + \sum_{n=n'-1}^{n'+1} p_n^{(x)} C_{n-n',\mathrm{SR}}^{\mathrm{TEM}_z,xx} \right.
$$

$$
\left. + \frac{1}{c_0} \sum_{n=0}^{N-1} m_n^{(y)} D_{n-n',\mathrm{LR}}^{\mathrm{TEM}_z,yx} \right] + \alpha_E^{xx} \varepsilon_0 E_{inc,x} e^{-jk_0 dn'},
$$

$$
\forall n' = 0, 1, 2, \ldots, N-1 \quad (28)
$$

$$
m_{n'}^{(y)} = \frac{\alpha_M^{yy}}{(ab)^{3/2}} \left[c_0 \sum_{n=0}^{N-1} p_n^{(x)} D_{n-n',\mathrm{LR}}^{\mathrm{TEM}_z,yx} + \sum_{n=0}^{N-1} m_n^{(y)} C_{n-n',\mathrm{LR}}^{\mathrm{TEM}_z,xx} \right.
$$

$$
\left. + \sum_{n=n'-1}^{n'+1} m_n^{(y)} C_{n-n',\mathrm{SR}}^{\mathrm{TEM}_z,yy} \right] + \alpha_M^{yy} \frac{E_{inc,x}}{\eta_0} e^{-jk_0 dn'},
$$

$$
\forall \ n' = 0, 1, 2, \ldots, N-1 \quad (29)
$$

where in writing Eq. (29) we substituted $C_{n-n',\mathrm{LR}}^{\mathrm{TEM}_z,yy} = C_{n-n',\mathrm{LR}}^{\mathrm{TEM}_z,xx}$.

4. EIGENMODE EXPANSION

Equations (28) and (29) constitute a linear system of $2N$ equations for the $2N$ unknowns: $p_n^{(x)}$ and $m_n^{(y)}$; $n = 0, 1, 2, \ldots, N-1$. One way to solve this set of equations is simply by direct numerical computation, which involves numerically inverting the corresponding $2N \times 2N$ matrix of the coefficient of variables. Such an approach was taken by Berman [22] for the all-dielectric case and Shore and Yaghjian [45] for the case of magnetodielectric spherical particles. Here we take an alternative approach and solve the system of equations using the following expansion of polarization by eigenmodes:

$$
p_n^{(x)} = \sum_i P_{x,i}^+ e^{-jq_{z,i}dn} + P_{x,i}^- e^{+jq_{z,i}dn} \quad (30)
$$

$$
m_n^{(y)} = \sum_i M_{y,i}^+ e^{-jq_{z,i}dn} + M_{y,i}^- e^{+jq_{z,i}dn}, \quad (31)
$$

where $P_{x,i}^+$ and $M_{y,i}^+$ are the amplitudes of the eigenmodes traveling in the $+z$-direction with wavenumbers $q_{z,i}$; $P_{x,i}^-$ and $M_{y,i}^-$ are the amplitudes of the eigenmodes traveling in the $-z$-direction with wavenumbers $-q_{z,i}$; and $i = 1, 2, \ldots, I$, where I is the number of modes as determined by the number of roots of the dispersion relation. Each eigenmode (or Floquet wave) constitutes a "natural" solution

which can independently propagate through the corresponding infinite periodic structure with wavenumber $\pm q_{z,i}$.

Substituting Eqs. (30) and (31) into Eqs. (28) and (29) yields:

$$\sum_i \left(P_{x,i}^+ e^{-jq_{z,i}an'} + P_{x,i}^- e^{+jq_{z,i}an'} \right)$$

$$= \frac{\alpha_E^{xx}}{(ab)^{3/2}} \left\{ \sum_i P_{x,i}^+ \left(\sum_{n=0}^{N-1} e^{-jq_{z,i}dn} C_{n-n',\text{LR}}^{\text{TEM}_z,xx} + \sum_{n=n'-1}^{n'+1} e^{-jq_{z,i}dn} C_{n-n',\text{SR}}^{\text{TEM}_z,xx} \right) \right.$$

$$+ \sum_i P_{x,i}^- \left(\sum_{n=0}^{N-1} e^{+jq_{z,i}dn} C_{n-n',\text{LR}}^{\text{TEM}_z,xx} + \sum_{n=n'-1}^{n'+1} e^{+jq_{z,i}dn} C_{n-n',\text{SR}}^{\text{TEM}_z,xx} \right)$$

$$+ \frac{1}{c_0} \sum_i M_{y,i}^+ \left(\sum_{n=0}^{N-1} e^{-jq_{z,i}dn} D_{n-n',\text{LR}}^{\text{TEM}_z,yx} \right)$$

$$\left. + \frac{1}{c_0} \sum_i M_{y,i}^- \left(\sum_{n=0}^{N-1} e^{+jq_{z,i}dn} D_{n-n',\text{LR}}^{\text{TEM}_z,yx} \right) \right\}$$

$$+ \varepsilon_0 \alpha_E^{xx} E_{inc,x} e^{-jk_0 dn'}, \ \forall \ n' = 0, 1, 2, \ldots, N-1 \quad (32)$$

$$\sum_i \left(M_{y,i}^+ e^{-jq_{z,i}an'} + M_{y,i}^- e^{+jq_{z,i}an'} \right)$$

$$= \frac{\alpha_M^{yy}}{(ab)^{3/2}} \left\{ c_0 \sum_i P_{x,i}^+ \left(\sum_{n=0}^{N-1} e^{-jq_{z,i}dn} D_{n-n',\text{LR}}^{\text{TEM}_z,yx} \right) \right.$$

$$+ c_0 \sum_i P_{x,i}^- \left(\sum_{n=0}^{N-1} e^{+jq_{z,i}dn} D_{n-n',\text{LR}}^{\text{TEM}_z,yx} \right)$$

$$+ \sum_i M_{y,i}^+ \left(\sum_{n=0}^{N-1} e^{-jq_{z,i}dn} C_{n-n',\text{LR}}^{\text{TEM}_z,xx} + \sum_{n=n'-1}^{n'+1} e^{-jq_{z,i}dn} C_{n-n',\text{SR}}^{\text{TEM}_z,yy} \right)$$

$$\left. + \sum_i M_{y,i}^- \left(\sum_{n=0}^{N-1} e^{+jq_{z,i}dn} C_{n-n',\text{LR}}^{\text{TEM}_z,xx} + \sum_{n=n'-1}^{n'+1} e^{-jq_{z,i}dn} C_{n-n',\text{SR}}^{\text{TEM}_z,yy} \right) \right\}$$

$$+ \alpha_M^{xx} \frac{E_{inc,x} e^{-jk_0 dn'}}{\eta_0}, \ \forall \ n' = 0, 1, 2, \ldots, N-1 \quad (33)$$

We proceed next by evaluating one-by-one in closed-form the finite planewise sums over n which appear in Eqs. (32) and (33). First, let

us expand the sums involving short-range interactions:

$$\sum_{n=n'-1}^{n'+1} e^{\pm jq_{z,i}dn} C_{n-n',\text{SR}}^{\text{TEM}_z,xx}$$

$$= e^{\pm jq_{z,i}dn'} \left\{ \tilde{C}_{0,\text{SR}}^{\text{TEM}_z,xx} + 2C_{1,\text{SR}}^{\text{TEM}_z,xx} \cos(q_{z,i}d) - \delta_{n'0} C_{1,\text{SR}}^{\text{TEM}_z,xx} e^{\mp jq_{z,i}d} \right.$$

$$\left. - \delta_{n'(N-1)} C_{1,\text{SR}}^{\text{TEM}_z,xx} e^{\mp jq_{z,i}d} \right\} + j(ab)^{3/2} \frac{k_0^3}{6\pi} e^{\pm jq_{z,i}dn'} \tag{34}$$

$$\sum_{n=n'-1}^{n'+1} e^{\pm jq_{z,i}dn} C_{n-n',\text{SR}}^{\text{TEM}_z,yy}$$

$$= e^{\pm jq_{z,i}dn'} \left\{ \tilde{C}_{0,\text{SR}}^{\text{TEM}_z,yy} + 2C_{1,\text{SR}}^{\text{TEM}_z,yy} \cos(q_{z,i}d) - \delta_{n'0} C_{1,\text{SR}}^{\text{TEM}_z,yy} e^{\mp jq_{z,i}d} \right.$$

$$\left. - \delta_{n'(N-1)} C_{1,\text{SR}}^{\text{TEM}_z,yy} e^{\mp jq_{z,i}d} \right\} + j(ab)^{3/2} \frac{k_0^3}{6\pi} e^{\pm jq_{z,i}dn'} \tag{35}$$

where δ_{ij} is the Kronecker delta function ($\delta_{ij} = 1$ for $i = j$ and $\delta_{ij} = 0$ for $i \neq j$) and $\tilde{C}_{0,\text{SR}}^{\text{TEM}_z,xx}$ and $\tilde{C}_{0,\text{SR}}^{\text{TEM}_z,yy}$ are defined to be the respective interaction constants minus the radiation damping term:

$$\tilde{C}_{0,\text{SR}}^{\text{TEM}_z,xx} \equiv C_{0,\text{SR}}^{\text{TEM}_z,xx} - j(ab)^{3/2} k_0^3/6\pi = \text{Re}\left(C_0^{\text{TEM}_z,xx}\right) \tag{36}$$

$$\tilde{C}_{0,\text{SR}}^{\text{TEM}_z,yy} \equiv C_{0,\text{SR}}^{\text{TEM}_z,yy} - j(ab)^{3/2} k_0^3/6\pi = \text{Re}\left(C_0^{\text{TEM}_z,yy}\right). \tag{37}$$

Next, let us evaluate the planewise sums over n that appear in Eqs. (32) and (33) involving the long-range component $C_{n-n',\text{LR}}^{\text{TEM}_z,xx}$:

$$\sum_{n=0}^{N-1} e^{\pm jq_{z,i}dn} C_{n-n',\text{LR}}^{\text{TEM}_z,xx} = -j\frac{k_0(ab)^{1/2}}{2} \sum_{n=0}^{N-1} e^{\pm jq_{z,i}dn} e^{-j|n-n'|k_0 d}$$

$$= -j\frac{k_0(ab)^{1/2}}{2} \left\{ e^{-jk_0 dn'} \left[\frac{1}{1 - e^{j(\pm q_{z,i}+k_0)dn}} \right] \right.$$

$$\left. + e^{\pm jq_{z,i}dn'} \left[\frac{j\sin(k_0 d)}{\cos(k_0 d) - \cos(q_{z,i}d)} \right] - e^{+jk_0 dn'} \left[\frac{e^{-j(k_0-(\pm)q_{z,i})Nd}}{1 - e^{j(\pm q_{z,i}-k_0)d}} \right] \right\} \tag{38}$$

where we substituted Eq. (21) for $C_{n-n',\text{LR}}^{\text{TEM}_z,xx}$. Note that the final expression has been purposely expressed as a sum of terms proportional to $e^{-jk_0 dn'}$, $e^{+jk_0 dn'}$, and $e^{\pm jq_z dn'}$.

Next, let us evaluate the planewise sums over n that appear in

Eqs. (32) and (33) involving the long-range component $D_{n-n',\text{LR}}^{\text{TEM}_z,yx}$:

$$\sum_{n=0}^{N-1} e^{\pm jq_{z,i}dn} D_{n-n',\text{LR}}^{\text{TEM}_z,yx}$$

$$= \frac{jk_0 (ab)^{1/2}}{2} \sum_{n=0}^{N-1} \text{sgn}\,(n-n')\, e^{\pm jq_{z,i}dn} e^{-j|n-n'|k_0 d}$$

$$= \frac{jk_0 (ab)^{1/2}}{2} \left\{ \pm e^{\pm jq_{z,i}dn'} \left[\frac{j\sin(q_{z,i}d)}{\cos(k_0 d) - \cos(q_{z,i}d)} \right] \right.$$

$$\left. - e^{-jk_0 dn'} \left[\frac{1}{1 - e^{j(\pm q_{z,i}+k_0)dn}} \right] - e^{+jk_0 dn'} \left[\frac{e^{j(\pm q_{z,i}-k_0)Nd}}{1 - e^{j(\pm q_{z,i}-k_0)d}} \right] \right\} \quad (39)$$

where we substituted Eq. (26) for $D_{n-n',\text{LR}}^{\text{TEM}_z,yx}$, and, as in Eq. (38), the final expression has been expressed as a sum of terms proportional to $e^{-jk_0 dn'}$, $e^{+jk_0 dn'}$, and $e^{\pm jq_z dn'}$.

Substituting Eqs. (34), (35), (38), and (39) into Eqs. (32) and (33) yields a rather cumbersome set of local-field equations (not shown) governing the response of each plane in the system. In general, each equation involves a superposition of terms proportional to $e^{-jk_0 dn'}$, $e^{+jk_0 dn'}$, $e^{-jq_z dn'}$, and $e^{+jq_z dn'}$. Since both $q_{z,i}$ and k_0 are independent of both the planar index n' and the number of planes N, each of these terms in the equations must separately equal zero. Performing this grouping leads to the following "decoupled" set of equations which, all together, completely characterize the slab's electromagnetic response:

$$P_{x,i}^+ \left\{ \tilde{C}_{0,\text{SR}}^{\text{TEM}_z,xx} + 2C_{1,\text{SR}}^{\text{TEM}_z,xx} \cos(q_{z,i}d) - \left(\alpha_E'^{xx} \right)^{-1} (ab)^{3/2} \right.$$

$$\left. + \left(\frac{k_0 (ab)^{1/2}}{2} \right) \left(\frac{\sin(k_0 d)}{\cos(k_0 d) - \cos(q_{z,i}d)} \right) \right\}$$

$$+ M_{y,i}^+ \left\{ \frac{1}{c_0} \left(\frac{k_0 (ab)^{1/2}}{2} \right) \left(\frac{\sin(q_{z,i}d)}{\cos(k_0 d) - \cos(q_{z,i}d)} \right) \right\} = 0 \quad (40)$$

$$P_{x,i}^+ \left\{ c_0 \left(\frac{k_0 (ab)^{1/2}}{2} \right) \left(\frac{\sin(q_{z,i}d)}{\cos(k_0 d) - \cos(q_{z,i}d)} \right) \right\}$$

$$+ M_{y,i}^+ \left\{ \tilde{C}_{0,\text{SR}}^{\text{TEM}_z,yy} + 2C_{1,\text{SR}}^{\text{TEM}_z,yy} \cos(q_{z,i}d) - \left(\alpha_M'^{yy} \right)^{-1} (ab)^{3/2} \right.$$

$$\left. + \left(\frac{k_0 (ab)^{1/2}}{2} \right) \left(\frac{\sin(k_0 d)}{\cos(k_0 d) - \cos(q_{z,i}d)} \right) \right\} = 0 \quad (41)$$

$$P_{x,i}^- \left\{ \tilde{C}_{0,\text{SR}}^{\text{TEM}_z,xx} + 2C_{1,\text{SR}}^{\text{TEM}_z,xx} \cos(q_{z,i}d) - \left(\alpha_E^{'xx}\right)^{-1}(ab)^{3/2} \right.$$

$$\left. + \left(\frac{k_0 (ab)^{1/2}}{2}\right)\left(\frac{\sin(k_0 d)}{\cos(k_0 a) - \cos(q_{z,i}d)}\right)\right\}$$

$$-M_{y,i}^- \left\{\frac{1}{c_0}\left(\frac{k_0 (ab)^{1/2}}{2}\right)\left(\frac{\sin(q_{z,i}d)}{\cos(k_0 d) - \cos(q_{z,i}d)}\right)\right\} = 0 \quad (42)$$

$$-P_{x,i}^- \left\{ c_0 \left(\frac{k_0 (ab)^{1/2}}{2}\right)\left(\frac{\sin(q_{z,i}d)}{\cos(k_0 d) - \cos(q_{z,i}d)}\right)\right\}$$

$$+M_{y,i}^- \left\{ \tilde{C}_{0,\text{SR}}^{\text{TEM}_z,yy} + 2C_{1,\text{SR}}^{\text{TEM}_z,yy} \cos(q_{z,i}d) - \left(\boldsymbol{\alpha}_M^{'yy}\right)^{-1}(ab)^{3/2}\right.$$

$$\left. + \left(\frac{k_0 (ab)^{1/2}}{2}\right)\left(\frac{\sin(k_0 d)}{\cos(k_0 d) - \cos(q_{z,i}d)}\right)\right\} = 0 \quad (43)$$

$$\sum_i P_{x,i}^+ e^{+jq_{z,i}d} + P_{x,i}^- e^{-jq_{z,i}d} = 0 \quad (44)$$

$$\sum_i P_{x,i}^+ e^{-jq_{z,i}dN} + P_{x,i}^- e^{+jq_{z,i}dN} = 0 \quad (45)$$

$$\sum_i M_{x,i}^+ e^{+jq_{z,i}d} + M_{x,i}^- e^{-jq_{z,i}d} = 0 \quad (46)$$

$$\sum_i M_{x,i}^+ e^{-jq_{z,i}dN} + M_{x,i}^- e^{+jq_{z,i}dN} = 0 \quad (47)$$

$$\sum_i \left(P_{x,i}^+ + M_{y,i}^+\big/c_0\right)\left(\frac{1}{1 - e^{-j(q_{z,i}-k_0)d}}\right)$$

$$+ \left(P_{x,i}^- + M_{y,i}^-\big/c_0\right)\left(\frac{1}{1 - e^{-j(-q_{z,i}-k_0)d}}\right) = \frac{-j2ab\varepsilon_0 E_{inc,x}}{k_0} \quad (48)$$

$$\sum_i \left(P_{x,i}^+ - M_{y,i}^+\big/c_0\right)\left(\frac{e^{-j(k_0+q_{z,i})Nd}}{1 - e^{-j(q_{z,i}+k_0)d}}\right)$$

$$+ \left(P_{x,i}^- - M_{y,i}^-\big/c_0\right)\left(\frac{e^{-j(k_0-q_{z,i})Nd}}{1 - e^{j(q_{z,i}-k_0)d}}\right) = 0 \quad (49)$$

where, in Eqs. (40) – (43), we have defined

$$\left(\alpha_E^{'xx}\right)^{-1} \equiv (\alpha_E^{xx})^{-1} - jk_0^3/6\pi \quad (50)$$

$$\left(\alpha_M^{'yy}\right)^{-1} \equiv (\alpha_E^{yy})^{-1} - jk_0^3/6\pi, \quad (51)$$

Independent of whether the scatterers are lossy or not, the imaginary parts of $(\alpha_E^{xx})^{-1}$ and $(\alpha_M^{xx})^{-1}$ each contain the radiation damping term $+jk_0^3/6\pi$ [15, 24, 46]. In our definitions of $\left(\alpha_E'^{xx}\right)^{-1}$ and $\left(\alpha_M'^{yy}\right)^{-1}$ given by Eqs. (50) and (51), this radiation damping term is exactly canceled with its negative. Hence, $\alpha_E'^{xx}$ and $\alpha_M'^{yy}$ are recognized to be the polarizations computed without radiation damping.

Equations (40)–(43) describe the natural response of the structure and yield both the dispersion relation and the particular magnetic-to-electric amplitude ratios, $M_{y,i}^+/(c_0 P_{x,i}^+)$ and $M_{y,i}^-/(c_0 P_{x,i}^-)$, for each mode (see Section 5). As an alternative, we could have derived these same four homogeneous equations by analyzing the natural oscillations of a corresponding crystal of infinite extent using the Bloch-Floquet theory. Eqs. (44)–(47) are recognized to be the boundary conditions, and indicate that both the total electric and magnetic dipole moment distributions equal zero at two "fictitious" planes in the air-regions adjacent to the two boundaries of the slab (corresponding to fictitious planar indices $n = -1$ and $n = N$). This perhaps hints at a "natural" effective thickness to the equivalent continuous medium slab. Eqs. (48) and (49) constitute the forced response, and result by grouping terms proportional to $e^{-jk_0an'}$ and $e^{+jk_0an'}$ equal to zero in Eqs. (32) and (33). As such, Eqs. (48) and (49) can be regarded as the discrete analogs of the Ewald-Oseen extinction theorem for a magnetodielectric material slab. Eq. (48) tells us that in discrete space each eigenmode produces a field traveling plane-to-plane in the $+z$ direction with wavenumber k_0 such that the sum total over all such eigenmodes exactly cancels out the incident field, which also travels in the $+z$ direction with wavenumber k_0. Eq. (49) tells us that that each eigenmode also produces a field traveling in the $-z$ direction with wavenumber $-k_0$ such that the sum total over all such eigenmodes exactly cancels to zero (there is no incident field traveling in the $-z$ direction to be canceled out).

5. THE DISPERSION RELATION

Equations (40) and (41) constitute a 2×2 set of linear equations for the unknown amplitudes $P_{x,i}^+$ and $M_{y,i}^+$, while Eqs. (42) and (43) constitute a 2×2 set of linear equations for $P_{x,i}^-$ and $M_{y,i}^-$. So that a nontrivial solution exists, the matrix of the coefficient of variables for both sets of equations must each have a determinant equal to zero. By performing this operation and simplifying, we find that both sets of equations lead to the same dispersion relation as the infinite crystal (see Sections 6 in Ref. [44]) as expected. This dispersion relation can be written in the

form of a cubic equation with variable $\cos(q_{z,i}a)$:

$$Q_3 w^3 + Q_2 w^2 + Q_1 w + Q_0 = 0; \quad w = \cos(q_{z,i}d) \tag{52}$$

where the terms Q_1, Q_2, Q_2, and Q_0 are given by Eqs. (46)–(49) in Ref. [44]. By taking the inverse cosine of the roots of Eq. (52), the eigenvalues $q_{z,i}$ are found within a plus or minus sign. For the lossy case we choose the sign of $q_{z,i}$ corresponding to a negative imaginary component ($\text{Im}[q_{z,i}] < 0$). In this manner, the eigenmodes decay as they travel along the z-axis. For the lossless case, we choose the sign corresponding to positive energy transfer, such that $\partial q_{z,i}/\partial\omega > 0$. The dispersion relation given by Eq. (52) has precisely three roots because we included only nearest-neighbor near-field interactions in the analysis. In general, for magnetodielectric crystals in the case of normal incidence, including L neighboring near-field interactions results in a polynomial of degree $1 + 2L$. This is in contrast to an all-dielectric or all-magnetic structure in which the number of roots is $1 + L$ [29].

Each eigenmode has a set of fixed electric-to-magnetic amplitude ratios, denoted $B_{yx,i}^{\text{TEM}_z(+)} \equiv M_{y,i}^+/(c_0 P_{x,i}^+)$ and $B_{yx,i}^{\text{TEM}_z(-)} \equiv M_{y,i}^-/(c_0 P_{x,i}^-)$. Eq. (40) yields the following expression for $B_{yx,i}^{\text{TEM}_z(+)}$:

$$B_{yx,i}^{\text{TEM}_z(+)} = \frac{\tilde{C}_{0,\text{SR}}^{\text{TEM}_z,xx} + 2C_{1,\text{SR}}^{\text{TEM}_z,xx}\cos(q_{z,i}d) \\ -\left(\alpha_E'^{xx}\right)^{-1}(ab)^{3/2} + \frac{(k_0/2)(ab)^{1/2}\sin(k_0d)}{\cos(k_0d)-\cos(q_{z,i}d)}}{\left(\frac{k_0(ab)^{1/2}}{2}\right)\left(\frac{\sin(q_{z,i}d)}{\cos(q_{z,i}d)-\cos(k_0d)}\right)} \tag{53}$$

Eq. (41) yields an alternative equivalent expression for $B_{yx,i}^{\text{TEM}_z(+)}$. Additionally, from Eq. (42) and/or Eq. (43), we find:

$$B_{yx,i}^{\text{TEM}_z(-)} = -B_{yx,i}^{\text{TEM}_z(+)} \tag{54}$$

6. THE SCATTERING PARAMETERS

After substituting $M_{y,i}^+ = c_0 P_{x,i}^+ B_{yx,i}^{\text{TEM}_z(+)}$ and $M_{y,i}^- = -c_0 P_{x,i}^- B_{yx,i}^{\text{TEM}_z(-)}$ into Eqs. (46)–(49), we find that Eqs. (44)–(49) form a complete set of six linear equations, which can be solved for the six unknown amplitudes, $P_{x,i}^+$ and $P_{x,i}^-$; $i = 1, 2, 3$. For clarity, let us rewrite Eqs. (44)–(49) in the matrix form $[\mathbf{A}][\mathbf{x}]=[\mathbf{b}]$, where

$$[\mathbf{b}] = \left[0, 0, 0, 0, 0, \tilde{E}_{inc,x}\right]^T \tag{55}$$

$$[\mathbf{x}] = \left[P_{x,1}^+, P_{x,2}^+, P_{x,3}^+, P_{x,1}^-, P_{x,2}^-, P_{x,3}^- \right]^T \tag{56}$$

$$[\mathbf{A}] = \begin{bmatrix} e^{jq_{z,1}d} & e^{jq_{z,2}d} & e^{jq_{z,3}d} & e^{-jq_{z,1}d} & e^{-jq_{z,2}d} & e^{-jq_{z,3}d} \\ e^{-jq_{z,1}dN} & e^{-jq_{z,2}dN} & e^{-jq_{z,3}dN} & e^{jq_{z,1}dN} & e^{jq_{z,2}dN} & e^{jq_{z,3}dN} \\ F_1^+ & F_2^+ & F_3^+ & F_1^- & F_2^- & F_3^- \\ G_1^+ & G_2^+ & G_3^+ & G_1^- & G_2^- & G_3^- \\ H_1^+ & H_2^+ & H_2^+ & H_1^- & H_2^- & H_3^- \\ U_1^+ & U_2^+ & U_3^+ & U_1^- & U_2^- & U_3^- \end{bmatrix} \tag{57}$$

where, for compactness in notation, we have defined:

$$\tilde{E}_{inc,x} \equiv \frac{-j2ab\varepsilon_0 E_{inc,x}}{k_0} \tag{58}$$

$$F_i^\pm \equiv \pm B_{yx,i}^{\mathrm{TEM}_z} e^{\pm jq_{z,i}d} \tag{59}$$

$$G_i^\pm \equiv \pm B_{yx,i}^{\mathrm{TEM}_z} e^{-(\pm jq_{z,i}Nd)} \tag{60}$$

$$U_i^\pm \equiv \left(B_{yx,i}^{\mathrm{TEM}_z} \pm 1 \right) \left(\frac{1}{1 - e^{-j(\pm q_{z,i} - k_0)d}} \right) \tag{61}$$

$$H_i^\pm \equiv -\left(B_{yx,i}^{\mathrm{TEM}_z} \pm 1 \right) \left(\frac{e^{-j(k_0 \pm q_{z,i})Nd}}{1 - e^{-j(\pm q_{z,i} + k_0)d}} \right) \tag{62}$$

In practice, the matrix equation $[\mathbf{A}][\mathbf{x}] = [\mathbf{b}]$ can be solved by numerically inverting the 6×6 matrix of the coefficient of variables, $[\mathbf{A}]$, which is given by Eq. (57). For $N > 3$, this is a much more efficient calculation than directly solving for the plane-to-plane distributions, $p_n^{(x)}$ and $m_n^{(y)}$; $n = 0, 1, 2, \ldots, N - 1$, via numerically inverting the original $2N \times 2N$ matrix described by Eqs. (28) and (29). The exact difference in computational time and memory is dependent on N and the user's particular numerical inversion scheme.

The total scattered electric field in the first air region ($z < 0$) is a superposition of a reflected plane wave, which we denote $\mathbf{E}_r = \hat{\mathbf{a}}_x S_{11} E_{inc,x} e^{-jk_0|z|}$, and a combination of scattered evanescent waves produced by the lattice. For observation points a sufficient distance away (generally three lattice constants from the surface is adequate), the evanescent fields are negligible and the total scattered field is simply equal to that of the reflected plane wave $\mathbf{E}_r$. The reflection coefficient, S_{11}, is found by summing the contribution from each discrete scatterer in the array to the electric field amplitude of the scattered plane wave, and normalizing the field by $E_{inc,x}$. Taking a planewise summation

approach, the above statement can be expressed as follows:

$$
\begin{aligned}
S_{11} &= \frac{1}{E_{inc,x}\,(ab)^{3/2}\,\varepsilon_0} \sum_{n=0}^{N-1} p_n^{(x)} C_{n,\mathrm{LR}}^{\mathrm{TEM}_z,xx} - \frac{1}{c_0} m_n^{(y)} D_{n,\mathrm{LR}}^{\mathrm{TEM}_z,yx} \\
&= \frac{k_0}{j E_{inc,x}\varepsilon_0 2ab} \sum_{i=1}^{3} \sum_{n=0}^{N-1} P_{x,i}^{+} e^{-j(q_{z,i}+k_0)dn} \left(1 - B_{yx,i}^{\mathrm{TEM}_z}\right) \\
&\quad + P_{x,i}^{-} e^{-j(-q_{z,i}+k_0)dn} \left(1 + B_{yx,i}^{\mathrm{TEM}_z}\right) \\
&= \frac{-1}{\tilde{E}_{inc,x}} \sum_{i=1}^{3} P_{x,i}^{+} \frac{\left(1 - e^{-jdN(q_{z,i}+k_0)}\right)\left(1 - B_{yx,i}^{\mathrm{TEM}_z}\right)}{1 - e^{-j(q_{z,i}+k_0)d}} \\
&\quad + P_{x,i}^{-} \frac{\left(1 - e^{-jdN(-q_{z,i}+k_0)}\right)\left(1 + B_{yx,i}^{\mathrm{TEM}_z}\right)}{1 - e^{-j(-q_{z,i}+k_0)d}}
\end{aligned}
\tag{63}
$$

The total scattered electric field in the second air region ($z > dN - d$) is a superposition of a transmitted plane wave, which we denote $\mathbf{E}_t = \hat{\mathbf{a}}_x S_{21} E_{inc,x} e^{-jk_0|z|}$, and a combination of scattered evanescent waves produced by the lattice, all of which decay rapidly to zero with increasing distance from the structure. Taking a planewise summation approach, we calculate the transmission coefficient, S_{21}, as follows:

$$
\begin{aligned}
S_{21} &= \frac{1}{E_{inc,x}} \left[E_{inc,x} e^{-jdk_0(N-1)} + \frac{1}{(ab)^{3/2}\,\varepsilon_0} \sum_{n=0}^{N-1} p_n^{(x)} C_{n-(N-1),\mathrm{LR}}^{\mathrm{TEM}_z,xx} \right. \\
&\quad \left. - \frac{1}{c_0} m_n^{(y)} D_{n-(N-1),\mathrm{LR}}^{\mathrm{TEM}_z,yx} \right] \\
&= e^{-jdk_0(N-1)} \left[1 + \frac{k_0}{j E_{inc,x}\varepsilon_0 2ab} \sum_{i=1}^{3} \sum_{n=0}^{N-1} P_{x,i}^{+} e^{-j(q_{z,i}-k_0)dn} \left(1 + B_{yx,i}^{\mathrm{TEM}_z}\right) \right. \\
&\quad \left. + P_{x,i}^{-} e^{+j(q_{z,i}+k_0)dn} \left(1 - B_{yx,i}^{\mathrm{TEM}_z}\right) \right] \\
&= e^{-jdk_0(N-1)} \left[1 + \frac{-1}{\tilde{E}_{inc,x}} \sum_{i=1}^{3} P_{x,i}^{+} \frac{\left(1 - e^{-jdN(q_{z,i}-k_0)}\right)\left(1 + B_{yx,i}^{\mathrm{TEM}_z}\right)}{1 - e^{-j(q_{z,i}-k_0)d}} \right. \\
&\quad \left. + P_{x,i}^{-} \frac{\left(1 - e^{+jdN(q_{z,i}+k_0)}\right)\left(1 - B_{yx,i}^{\mathrm{TEM}_z}\right)}{1 - e^{+j(q_{z,i}+k_0)d}} \right]
\end{aligned}
\tag{64}
$$

7. HFSS SIMULATION AND COMPARISON

In this section, we compare the reflection coefficient, S_{11}. and transmission coefficient, S_{21}, of a metamaterial slab calculated using the method presented in this paper with that obtained by full-wave simulation using Ansoft HFSS. Consider a metamaterial composed of a cubic lattice of magnetodielectric cubes. The lattice period $d = 1\,\text{cm}$ and the edge length of the cube is $0.76\,\text{cm}$. As a hypothetical material, we choose the relative permittivity ε_r and relative permeability μ_r of the magnetodielectric cube to be $\text{Re}(\varepsilon_r) = 65$ and $\text{Re}(\mu_r) = 40$ with loss tangents of $\tan\delta_E = \tan\delta_M = 5E-4$. Fig. 2 shows the geometric model and boundaries of the HFSS simulation for a single planar array of such cubes. Perfect electric conductor (PEC) and perfect magnetic conductor (PMC) boundaries are placed at appropriate symmetry planes such that the quarter-cube and its infinite number of images are equivalent to a $d \times d$ square array of whole cubes with an excitation corresponding to a normally incident plane wave. A stack of N arrays is built by cascading N unit cells along the z-axis. For large N, such a simulation can require a considerable amount of computation time and memory requirements. In contrast, our analytical approach is much more efficient, because it requires only the electric and magnetic polarizabilities; both of which can be found using the retrieval method of Ref. [15] involving the simulated response of just a single planar array.
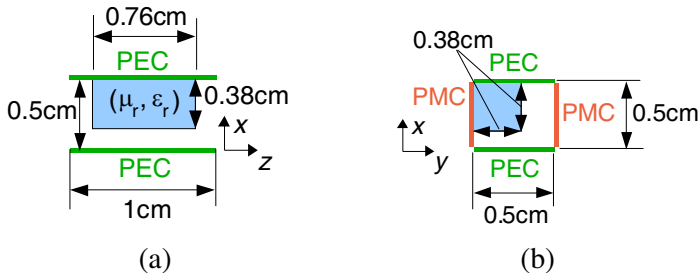

Figure 2. (a) xy-cross section and (b) xz-cross section of the HFSS model used to simulate the response of a planar array of magnetodielectric cubes to a normally incident plane wave. A metamaterial slab is modeled by cascading unit cells along the z-axis.

Figure 3 shows the extracted electric and magnetic polarizability densities for the structure using the method of Ref. [15] in the frequency range: $0.8\,\text{GHz}$–$1\,\text{GHz}$. As can be seen, the first resonance is magnetic and occurs around $0.905\,\text{GHz}$. The second resonance is electric and
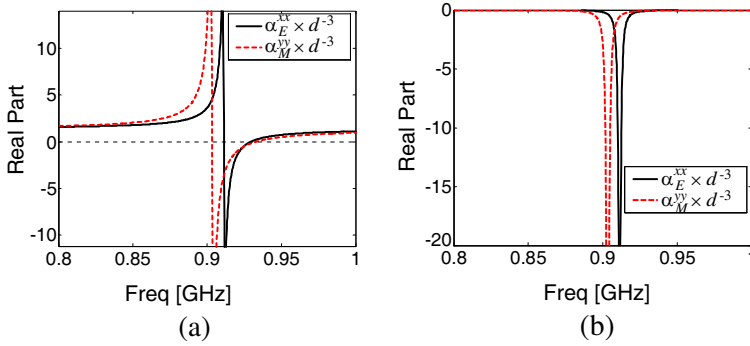
Figure 3. (a) Real and (b) imaginary polarization densities for a metamaterial composed of a cubic array of magnetodielectric cubes found via simulating a single array with HFSS and applying the scattering parameters to the retrieval method presented in Ref. [15].
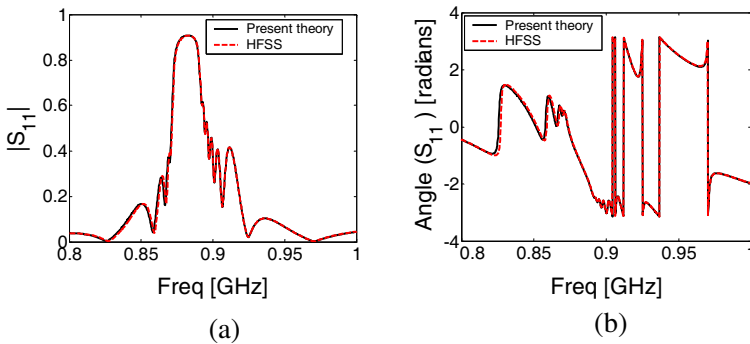

Figure 4. (a) Magnitude and (b) phase of S_{11} for a slab composed of seven layers ($N = 7$). The polarizability densities utilized in the calculations are shown in Figure 3.

occurs around $0.912\,\mathrm{GHz}$. Fig. 4 compares S_{11} for $N = 7$ as determined using our method to that obtained by simulating the full seven-layered structure in HFSS. As can be seen, our method agrees very well with the HFSS results; similarly, we also find good agreement for S_{21} (not shown). This case demonstrates the accuracy of our method, and validates the use of the point-dipole interaction model and nearest-neighbor approximation. This example demonstrated the major benefit of our theory, which is to accurately calculate the S_{11} and S_{21} response of a multi-layered slab (the particular number of layers is arbitrary) by simply knowing the polarizabilites of the individual

inclusions. If the polarizablities are unknown then they can be found first using an electromagnetic solver like HFSS in conjunction with a numerical extraction technique such as that presented in reference [15]. In general, extracting the polarizabilities of an individual scatterer uses much less memory and computation time than simulating a full multi-layered slab.

8. SUMMARY AND CONCLUSIONS

In this work, we solved for the electromagnetic response of a metamaterial slab in the case of normal incidence using the point-dipole interaction model and an expansion of polarization by eigenmodes. The problem was simplified considerably by assuming the lattice dimensions to be smaller than a wavelength and invoking the nearest neighbor approximation. In the future, we intend on expanding on these results to the case of oblique incidence. For ease of reference, below we summarize the steps developed in this paper for computing the reflection coefficient, S_{11}, and transmission coefficient, S_{21}, given the driving frequency, and the lattice dimensions, a, b, and d:

1. Compute the interaction constants $\tilde{C}_{0,\mathrm{SR}}^{\mathrm{TEM}_z,xx}(k_0, a, b)$ and $\tilde{C}_{0,\mathrm{SR}}^{\mathrm{TEM}_z,yy}(k_0, a, b) = \tilde{C}_{0,\mathrm{SR}}^{\mathrm{TEM}_z,xx}(k_0, b, a)$ using Eq. (36) in conjunction with Eq. (13) given in Ref. [44]. Compute $C_{1,\mathrm{SR}}^{\mathrm{TEM}_z,xx}(k_0, a, b, d)$ and $C_{1,\mathrm{SR}}^{\mathrm{TEM}_z,yy}(k_0, a, b, d) = C_{1,\mathrm{SR}}^{\mathrm{TEM}_z,xx}(k_0, b, a, d)$ using Eq. (22). For high accuracy, it is recommended to take at least twenty terms in each series.

2. Compute the frequency-dependent polarizability dyadics of the individual inclusions ($\overleftrightarrow{\boldsymbol{\alpha}}_{\mathrm{E}}$ and $\overleftrightarrow{\boldsymbol{\alpha}}_M$). If a closed form expressions for the polarizabilities don't exist, an electromagnetic solver like HFSS can be used in conjunction with a numerical extraction technique, such as the extraction technique presented in Ref. [15].

3. Solve the dispersion relation Eq. (52) for the eigenvalues, $q_{z,i}$; $i = 1, 2, 3$, and compute the electric-to-magnetic amplitude ratios, $B_{yx,i}^{\mathrm{TEM}_z(+)}$ and $B_{yx,i}^{\mathrm{TEM}_z(-)}$; $i = 1, 2, 3$, using Eqs. (53) and (54), respectively.

4. Find the amplitudes, $P_{x,i}^+$ and $P_{x,i}^-$; $i = 1, 2, 3$, by solving the 6×6 matrix equation $[\mathbf{A}][\mathbf{x}] = [\mathbf{b}]$ described by Eqs. (55–57). For convenience, set $\tilde{E}_{inc,x} = 1$.

5. Evaluate Eq. (63) for S_{11} and Eq. (64) for S_{21}.

REFERENCES

1. Pendry, J. B., "Negative refraction makes a perfect lens," *Physical Review Letters*, Vol. 85, 3966–3969, Oct. 30, 2000.

2. Maystre, D. and S. Enoch, "Perfect lenses made with left-handed materials: Alice's mirror?," *Journal of the Optical Society of America A — Optics Image Science and Vision*, Vol. 21, 122–131, Jan. 2004.

3. Larkin, I. A. and M. I. Stockman, "Imperfect perfect lens," *Nano Letters*, Vol. 5, 339–343, Feb. 2005.

4. Smith, D. R., D. Schurig, M. Rosenbluth, S. Schultz, S. A. Ramakrishna, and J. B. Pendry, "Limitations on subdiffraction imaging with a negative refractive index slab," *Applied Physics Letters*, Vol. 82, 1506–1508, Mar. 2003.

5. French, O. E., K. I. Hopcraft, and E. Jakeman, "Perturbation on the perfect lens: The near-perfect lens," *New Journal of Physics*, Vol. 8, 271, Nov. 13, 2006.

6. Merlin, R., "Analytical solution of the almost-perfect-lens problem," *Applied Physics Letters*, Vol. 84, 1290–1292, Feb. 23, 2004.

7. Enoch, S., G. Tayeb, P. Sabouroux, N. Guerin, and P. Vincent, "A metamaterial for directive emission," *Physical Review Letters*, Vol. 89, 213902-1–213902-4, Nov. 2002.

8. Alu, A., F. Bilotti, N. Engheta, and L. Vegni, "Metamaterial covers over a small aperture," *IEEE Transactions on Antennas and Propagation*, Vol. 54, 1632–1643, Jun. 2006.

9. Li, B., B. Wu, and C. H. Liang, "Study on high gain circular waveguide array antenna with metamaterial structure," *Progress In Electromagnetics Research*, Vol. 60, 207–219, 2006.

10. Saenz, E., K. Guven, E. Ozbay, I. Ederra, and R. Gonzalo, "Enhanced directed emission from metamaterial based radiation source," *Applied Physics Letters*, Vol. 92, 204103-1–204103–3, May 2008.

11. Engheta, N., "An idea for thin subwavelength cavity resonators using metamaterials with negative permittivity and permeability," *IEEE Antennas and Wireless Propagation Letters*, Vol. 1, 10–13, 2002.

12. Caiazzo, M., S. Maci, and N. Engheta, "A metamaterial surface for compact cavity resonators," *IEEE Antennas and Wireless Propagation Letters*, Vol. 3, 261–264, 2004.

13. Holloway, C. L., D. C. Love, E. F. Kuester, A. Salandrino, and N. Engheta, "Sub-wavelength resonators: On the use of metafilms

to overcome the lambda/2 size limit," *IET Microw. Antennas Propag.*, Vol. 2, 120–129, Mar. 2008.

14. Bilotti, F., L. Nucci, and L. Vegni, "An SRR based microwave absorber," *Microwave and Optical Technology Letters*, Vol. 48, 2171–2175, Nov. 2006.

15. Scher, A. D. and E. F. Kuester, "Extracting the bulk effective parameters of a metamaterial via the scattering from a single planar array of particles," *Metamaterials*, Vol. 3, No. 1, 44–55, 2009.

16. Simovski, C. R. and S. A. Tretyakov, "Local constitutive parameters of metamaterials from an effective-medium perspective," *Physical Review B*, Vol. 75, 195111-1–195111-10, May 2007.

17. Smith, D. R., S. Schultz, P. Markos, and C. M. Soukoulis, "Determination of effective permittivity and permeability of metamaterials from reflection and transmission coefficients," *Physical Review B*, Vol. 65, 195104-1–195104-5, May 15, 2002.

18. Smith, D. R., D. C. Vier, T. Koschny, and C. M. Soukoulis, "Electromagnetic parameter retrieval from inhomogeneous metamaterials," *Physical Review E*, Vol. 71, 036617-1–036617-11, Mar. 2005.

19. Kar, N. and A. Bagchi, "Local-field effect near the surface of dipolar lattices," *Solid State Communications*, Vol. 33, 645–648, 1980.

20. Poppe, G. P. M. and C. M. J. Wijers, "Exact solution of the optical-response of thick slabs in the discrete dipole approach," *Physica B*, Vol. 167, 221–237, Dec. 1990.

21. Clercx, H. J. H. and G. Bossis, "Electrostatic interactions in slabs of polarizable particles," *Journal of Chemical Physics*, Vol. 98, 8284–8293, May 1993.

22. Berman, D. H., "An extinction theorem for electromagnetic waves in a point dipole model," *American Journal of Physics*, Vol. 71, 917–924, Sep. 2003.

23. Sivukhin, D. V., "Molecular theory of the reflection and refraction of light," *Zh. Eksp. Teor. Fiz.*, Vol. 18, 976–994, 1948.

24. Scher, A. D., "Boundary effects in the electromagnetic metamaterial using the point-dipole interaction model," Ph.D. Dissertation, University of Colorado at Boulder, 2008.

25. Belov, P. A. and C. R. Simovski, "Homogenization of electromagnetic crystals formed by uniaxial resonant scatterers," *Physical Review E*, Vol. 72, 026615-1–026615-15, Aug. 2005.

26. Silveirinha, M. G., "Generalized Lorentz-Lorenz formulas for microstructured materials," *Physical Review B*, Vol. 76, 245117-

1–245117-9, Dec. 2007.

27. Silveirinha, M. G., "Metamaterial homogenization approach with application to the characterization of microstructured composites with negative parameters," *Physical Review B*, Vol. 75, 115104-1–115104-15, Mar. 2007.

28. Ewald, P. P., *On the Foundations of Crystal Optics*, Air Force Cabridge Research Laboratories, 1970.

29. Mahan, G. D. and G. Obermair, "Polaritons at surfaces," *Physical Review*, Vol. 183, 834–841, 1969.

30. Philpott, M. R., "Reflection of light by a semi-infinite dielectric," *Journal of Chemical Physics*, Vol. 60, 1410–1419, 1974.

31. Philpott, M. R., "Polaritons in a spatially dispersive dielectric half space," *Physical Review B*, Vol. 14, 3471–3487, 1976.

32. Philpott, M. R., "Effect of spatial dispersion of S-polarized optical properties of a slab dielectric," *Journal of Chemical Physics*, Vol. 60, 2520–2529, 1974.

33. Gadomsky, O. N. and K. V. Krutitsky, "Near-field effect in surface optics," *Journal of the Optical Society of America B — Optical Physics*, Vol. 13, 1679–1690, Aug. 1996.

34. Krutitsky, K. V. and S. V. Suhov, "Near-field effect in classical optics of ultra-thin films," *Journal of Physics B — Atomic Molecular and Optical Physics*, Vol. 30, 5341–5358, Nov. 1997.

35. Simovski, C. R., P. A. Belov, and M. S. Kondratjev, "Electromagnetic interaction of chiral particles in three-dimensional arrays," *Journal of Electromagnetic Waves and Applications*, Vol. 13, No. 2, 189–204, 1999.

36. Belov, P. A. and C. R. Simovski, "Oblique propagation of electromagnetic waves in regular 3D lattices of scatterers (dipole approximation)," *Proc. SPIE*, Vol. 4073, 266–276, 2000.

37. Gadomskii, O. N. and S. V. Sukhov, "Microscopic theory of a transition layer on the ideal surface of semiinfinite dielectric media and the near-field effect," *Optics and Spectroscopy*, Vol. 89, 261–267, Aug. 2000.

38. Simovski, C. R., M. Popov, and S. L. He, "Dielectric properties of a thin film consisting of a few layers of molecules or particles," *Physical Review B*, Vol. 62, 13718–13730, Nov. 15, 2000.

39. Tretyakov, S. A. and A. J. Viitanen, "Plane waves in regular arrays of dipole scatterers and effective-medium modeling," *Journal of the Optical Society of America A — Optics Image Science and Vision*, Vol. 17, 1791–1797, Oct. 2000.

40. Simovski, C. R. and S. L. He, "Frequency range and

explicit expressions for negative permittivity and permeability for an isotropic medium formed by a lattice of perfectly conducting omega particles," *Physics Letters A*, Vol. 311, 254–263, May 12, 2003.

41. Simovski, C. R., "Bloch material parameters of magneto-dielectric metamaterials and the concept of Bloch lattices," *Metamaterials*, Vol. 1, 62–80, 2007.

42. Simovski, C. R., "Analytical modelling of double-negative composites," *Metamaterials*, Vol. 2, 169–185, 2008.

43. Belov, P. A. and C. R. Simovski, "Boundary conditions for interfaces of electromagnetic crystals and the generalized Ewald-Oseen extinction principle," *Physical Review B*, Vol. 73, 045102-1–045102-14, Jan. 2006.

44. Scher, A. D. and E. F. Kuester, "Boundary effects in the electromagnetic response of a metamaterial in the case of normal incidence," *Progress In Electromagnetics Research B*, Vol. 14, 341–381, 2009.

45. Shore, R. A. and A. D. Yaghjian, "Electromagnetic waves on partially finite periodic arrays of lossless or lossy penetrable spheres," *IEICE Transactions on Communications*, Vol. E91b, 1819–1824, Jun. 2008.

46. Sipe, J. E. and J. V. Kranendonk, "Macroscopic electromagnetic theory of resonant dielectrics," *Physical Review A*, Vol. 9, 1806–1822, 1974.